ERJ
Engineering Research Journal
Faculty of Engineering
Minoufiya University

EFFECT OF OPERATING CONDITIONS ON WALL CONCENTRATION OF RO SYSTEMS

H. Kotb, E. H. Amer and K. A. Ibrahim

Mechanical Power Engineering Department, Faculty of Engineering, Menoufiya University, Shebin El-Kom, Egypt.

ABSTRACT

Desalination using reverse osmosis membranes has become very popular for producing fresh water from brackish and sea water. Concentration polarization occurs in any pressure driven membrane separation process. It describes an increase in the concentration at the membrane wall due to the rejection of ionic species transported there by the convective flux. Accurate prediction of concentration polarization (CP) phenomenon is critical for properly designing reverse osmosis (RO) processes because it enhances transmembrane osmotic pressure and solute passage, as well as surface fouling and scaling phenomena. Membrane life time and permeate flux, however, are primarily affected by the phenomena of concentration polarization and fouling at the membrane surface. This paper aims to investigate the effect of the following parameters on concentration polarization phenomenon such as; feed specifications (flow rate and concentration), operating conditions (feed pressure and temperature) and Membrane dimensions (length and diameter).

ان تحليه المياه بشكل عام هى وسيلة لإزالة الملح من مياه البحر أو المياه الماثله للملوحه عموما. وتعتبر عمليه التحليه بالتناضح العكسى من أكثر عمليات التحليه المستخدمه، اذ تعتبر عملية التحليه بالتناضح العكسى الأفضل اقتصاديا لتحلية المياه المالحه باعتبارها واحده من العمليات المقبوله على نطاق واسع، فان عملية التحليه بالتناضح العكسى أصبحت منافس قوى وأكثر تفوقا على عمليات التحليه الحراريه التقليديه عند مقارنتها من ناحية استهلاك الطاقه. ومن الظواهر المؤثره فى أداء منظومة التحليه بالتناضح العكسى عملية تبلور الملح على جدار الغشاء جهة مياه التغذيه وذلك بسبب الزياده الكبيره فى تركيز المياه فى المنطقه الجداريه الملامسه للغشاء، هذه الظاهره تؤدى الى انخفاض معدل المياه العذبه الناتجه من الوحده وكذلك زيادة تركيز الأملاح فى هذه المياه وكذلك انخفاض العمر الافتراضى للغشاء. وللتغلب على هذة المشكله كان لابد من دراسة تأثير العوامل المختلفه عليها وذلك للحد من تأثيرها.

يتضمن هذا البحث دراسه نظريه لجميع التركيبات المختلفه التى يمكن الحصول عليها فى نظام التحليه بالتناضح العكسى الذى يتكون من مرحلتين. والنموذج الرياضى المستخدم فى هذا البحث تم عرضه وتوضيحه والتأكد من دقة النتائج التى يمكن الحصول عليها منه فى بحث سابق [١٣]، باستخدام هذا النموذج يتم دراسة تأثير كل من مواصفات مياه التغذيه (معدل التصرف والتركيز) وكذلك ظروف التشغيل (الضغط ودرجة الحراره) وأيضا أبعاد الغشاء (الطول والقطر) على تركيز الملح عند جدار الغشاء.

Keywords: Reverse osmosis, Two-module, Operating Condition, Concentration polarization, Tubular Module.

1. INTRODUCTION

Water is one of the most abundant resources on earth, covering three-quarters of the planet's surface. However, about 97% of the earth's water is salt water in the oceans, and a tiny 3% is fresh water. This small percentage of the earth's water-which supplies most of human and animal needs-exists in ground water, lakes and rivers. Nearly, 70% from this tiny 3% of the world's fresh water is frozen in glaciers, permanent snow cover, ice and permafrost. Thirty percent of all fresh water is underground, most of it in deep, hard-to-reach aquifers. Lakes and rivers together contain just a little more than 0.25% of all fresh water; lakes contain most of it, [1]. Desalination using reverse osmosis membranes has become very popular for producing in fresh water from brackish and sea water. Membrane life time and permeate flux, however, are primarily affected by the phenomena of concentration polarization and fouling at the membrane surface, [2]. Concentration polarization occurs in any pressure driven membrane separation process. It describes an increase in the concentration at the membrane wall due to the rejection of ionic species transported there by the convective flux. It is an undesirable phenomenon which results in the increase of the osmotic pressure at the membrane wall and consequently, a reduction in the permeate flux and the membrane rejection coefficient, figure (1) shows the Schematic Diagram of the salt Fluxes across RO Membranes [3].

A number of investigators have carried out the work on different aspects of reverse osmosis sea water

desalination. Al-Bastaki and Abbas, [4] have used a simple model to predict the performance of hollow fiber RO membranes. Later, they studied the effect of ignoring concentration polarization and pressure drops on the recovery and the salt rejection, [5]. They found that ignoring concentration polarization and pressure drops results in significant overestimation of the recovery. Kim and Hoek, [6] have investigated this study to compare available analytical concentration polarization (CP) models to a more rigorous numerical model and experimental data. Predictions of local concentration polarization, permeate flux, and solute rejection by film theory and the numerical model also agreed well for realistic ranges of RO process operating conditions.

Zhou, et. al, [7] have studied the development of concentration polarization in a spiral wound reverse osmosis membrane channel and the depolarization effect of spacers are important concerns for understanding the performance of membrane processes. The simulation results demonstrated that the model developed in their study was a feasible way to estimate concentration polarization in spiral wound modules. Excellent fitness was found between the numerical simulations and experimental observations of the average permeate fluxes in along membrane channel of spiral wound membrane modules. Wardeh and Morvan, [8] have carried out computational fluid dynamics (CFD) simulations for fluid flow through rectangular channels filled with spacers. In order to, understand the effect of the spacers on the increase of shear stress on the membrane surface, study the reduction of precipitated salt on the membrane surface and monitor, the mass transfer performance across the membrane surface, a computational model that includes all of the important physical processes occurring in membrane systems are required. Results suggest that the zigzagging spacers' type is more desirable comparing with the submerged one in maintaining the membrane and desalination system performance. Goztilvez et al., [9] have proposed reverse osmosis system with recirculation (RRO) to evaluate the efficiency and to determine the situations where it can be preferable compared to other configurations or unit operations. Theoretically it is possible to obtain a high recovery with a system like that for saline water allowing the transport of the concentrated brines to the sea, but the economy of the process will depend on energy and equipment expenses. Jamal et al., [10] have simulated a model to develop and verify a small-scale reverse osmosis system. Their results indicated that; the model developed without concentration polarization was effectively used for the prediction of feed concentration; permeate concentration, rejection and flux as a function of operating time. Djebedjian et. al, [11] have investigated the effect of the feed water temperature, the feed pressure, the inlet acidity measure (pH) and the feed water salinity on the performance of a small-size brackish water reverse osmosis (RO) desalination test-rig. In the rang of experimental runs, the maximum gain in recovery ratio has been obtained from the feed water pressure increase. The increase of feed water temperature or pressure results in a recovery ratio increase while the increase of feed water salinity or feed water pH leads to a decrease in recovery ratio. Elguera and Perez Baez, [12] have developed the most adequate pre-treatment for high capacity seawater desalination plants with open intake. This has been attempted to show how important the adequate system for optimization of the pre-treatment system of seawater desalination plants of open intake. The results obtained with the application was reduced the operating costs of the desalination plants which treat this kind of water. The total benefits will increase in direct proportion to the amount of capacity installed in the desalination plants.

The present paper aims to develop a mathematical model of two-module reverse osmosis system for brackish and sea water. This model is suitable for all two-module arrangements. Effects of feed specifications (feed flow rate and feed concentration), operating conditions (feed pressure and feed temperature) and membrane dimensions (membrane length and membrane channel diameter) on the concentration polarization on membrane wall in each module are studied.

2. TWO-MODULE RO SYSTEM ARRANGEMENTS

Several arrangements of two-module feed forward RO systems with and without bypass streams and energy recovery were investigated as shown in figure (2). The membrane module is modeled as a tube side feed flow tubular module. A superstructure that incorporates all possible arrangements for two module feed forward RO systems is developed in figure (3). This superstructure is used to develop the general mathematical model for the RO system which can be used to simulate any of the module arrangements shown in figure (2).

3. SYSTEM REPRESENTATION

The quantity and concentration of the water needed to the second module according to the following equations, [13]:

$$Q_{f2} = X_f \times Q_f + X_r \times Q_{r1} + X_p \times Q_{p1} \qquad (1)$$

$$C_{f2} = \frac{X_f \times Q_f \times C_f + X_r \times Q_{r1} \times C_{r1}}{Q_{f2}} + \frac{X_p \times Q_{p1} \times C_{p1}}{Q_{f2}} \qquad (2)$$

The second module could be fed directly from the feed stream. It could also be fed by the retentate or permeate emerging from the first module.

For example, in figure (2-a), all the feed stream flows into the first module. Then, all the retentate of the first module goes directly to the second module. Finally, the permeate of the two modules are mixed to give the output. This can be obtained from the superstructure by putting both Xf and Xp equal to zero and setting Xr=1. Accordingly, all candidate designs could be deduced from the superstructure employing the values for split ratios presented in table [1].

All arrangements can be divided into two main groups. The first group targets the retentate. The retentate of the first module is either splitted or taken as it is and admitted to the second module for reprocessing. Thus, the group is called retentate reprocessing arrangement. It includes designs for the system given in figure (2-a) to (2-e) where the arrangement, given in figure (2-b), has a special case where the feed is divided over the two modules. The value of permeate split ratio (Xp) is equal to zero in this group. The second group designs for figure (2-f) to (2-i) and is called permeate re-processing arrangements. In this group the value of retentate split ratio (Xr) equals zero.

4. MATHEMATICAL MODEL OF UNIT OPERATIONS

A mathematical model describing the whole RO system has been derived. The model based on mass material and energy balances for the superstructure shown in figure (3). The balance equations have been calculated separately for each unit in operation. Membrane modules, pumps, mixers and splitters with complete information about the unit operations and stream properties are considered and then, effects of feed specifications (feed flow rate and feed concentration), operating conditions (feed pressure and feed temperature) and membrane dimensions (membrane length and membrane channel diameter) on the salt concentration on membrane wall in each module are investigated.

The RO system model discussed and verified previously by authors in ref. [13] will be used here.

4.1. Membrane Module

The membrane module shown in figure (4), The mass balance for the membrane is given by

$$Q_p = j_w \times A \tag{3}$$

The volume flow rate of retantate could be calculated as follows:

$$Q_r = Q_f - Q_P \tag{4}$$

The material balance for the membrane modules is expressed as:

$$R = 1 - \frac{C_p}{C_f} \tag{5}$$

The retentate concentration is computed as:

$$C_r = \frac{C_f \times Q_f - C_p \times Q_p}{Q_r} \tag{6}$$

The energy balance for the membrane module is written as:

$$P_r = P_f - \Delta P_{in} - \Delta P_{out} - \Delta P_f \tag{7}$$

The flux through the membrane is calculated, [14]

$$j_w = A_m \times P_{eff} \tag{8}$$

The concentration on the feed side membrane wall can be calculated as follows, [14]

$$C_w = C_p + \left(\frac{C_f + C_r}{2} - C_p \right) e^{\frac{j}{k}} \tag{9}$$

Residual transmembrane pressure can be obtained from the following equation, [14]

$$P_{eff} = \left(P_f - P_p - \Delta P_{in} - \frac{\Delta P_f}{2} \right) - \left(\pi_w - \pi_p \right) \tag{10}$$

Equations (8) to (10) can be used for tube side feed flow tubular and hollow fiber modules as well as spiral wound module.

The osmotic pressure (π) in Pa as a function of the salt concentration and temperature may be given as in [15] as follows;

$$\pi(C,T) = (0.6955 + 0.0025T) \times 10^8 \frac{C}{\rho} \tag{11}$$

The mass transfer coefficient (k) is calculated using the following equations, [16]:

For laminar flow (Re$\leq$ 2100)

$$k = 1.62 \times \left(\frac{\mathrm{Re} \times Sc \times d_{ch}}{l_{ch}} \right)^{0.33} \times \frac{D_s}{d_{ch}} \tag{12}$$

For turbulent flow (Re> 2100)

$$k = 0.023 \times \mathrm{Re}^{0.875} \times Sc^{0.25} \times \frac{D_s}{d_{ch}} \tag{13}$$

The pressure drop in the membrane module consists of pressure losses in the inlet and outlet module manifolds (ΔP_{in} and ΔP_{out}) and inside the membrane channel (ΔP_f). Pressure drop in the membrane channel is calculated using the fanning equation, [17].

$$\Delta P_f = 2 \times f \times \rho \times V_{ch}^2 \times \frac{l_{ch}}{d_{ch}} \tag{14}$$

Then f (fanning friction factor) is a function of the Reynolds number (Re), approximated with the relations for smooth bore pipes, [17]:

For laminar flow (Re≤2100):

$$f = \frac{16}{\mathrm{Re}} \tag{15}$$

For turbulent flow (Re> 2100)

$$f = \frac{0.0791}{\mathrm{Re}^{0.25}} \tag{16}$$

The density of sea water is computed as follows, [15]

$$\rho = 498.4m + \sqrt{248400m^2 + 752.4mC} \tag{17}$$

Where

$$m = 1.0069 - 2.757\times10^{-4}T \tag{18}$$

The viscosity of sea water in Pa.s is expressed as, [15]

$$\mu = 1.234\times10^{-6}\exp\left(0.00212C + \frac{1965}{(T+273.15)}\right) \tag{19}$$

The diffusivity of seawater in m^2/s is given as in [15] as follows;

$$D_s = 6.725\times10^{-6}\exp\left(0.1546\times10^{-3}C - \frac{2513}{(T+273.15)}\right) \tag{20}$$

Pressure drop in the inlet module manifold is treated as a series of sudden expansions from the feed pipeline into the module shell and sudden contractions from the module shell into each membrane channel. Similarly, pressure drop in the outlet module manifold is a series of sudden expansions from the membrane channel into the module shell and sudden contraction from the module shell into retentate pipeline. The general pressure drop equations for sudden expansions (ΔP_{ex}) and contractions (ΔP_{co}), [17] are:

$$\Delta P_{ex} = \left(1 - \frac{A_1}{A_2}\right)^2 \frac{V^2\rho}{2\alpha} \tag{21}$$

$$\Delta P_{co} = 0.55\left(1 - \frac{A_1}{A_2}\right)^2 \frac{V^2\rho}{2\alpha} \tag{22}$$

Where:

α=1 for Re > 2100 and α=0.5 for Re ≤ 2100.

Combination and modification of these equations to suit inlet and outlet manifolds for tubular modules results in:

$$\Delta P_{in} = \left(\left(1 - \frac{A_p}{A_{sh}}\right)^2 V_p^2 + 0.55\left(1 - \frac{n\times A_{ch}}{A_{sh}}\right)^2 V_{ch}^2\right)\frac{\rho}{2\alpha} \tag{23}$$

$$\Delta P_{out} = \left(\left(1 - \frac{n\times A_{ch}}{A_{sh}}\right)^2 V_{ch}^2 + 0.55\left(1 - \frac{A_p}{A_s}\right)^2 V_p^2\right)\frac{\rho}{2\alpha} \tag{24}$$

4.2. Pump

There is no change in the flow rate or concentration of the stream leaving the pumps, thus:

$$Q_o = Q_i \tag{25}$$

$$C_o = C_i \tag{26}$$

The pump efficiency is assumed to be 65%, [16]:

$$W_p = Q_i\frac{P_o - P_i}{0.65} \tag{27}$$

4.3. Mixer

The mass balance for a mixer is expressed using figure (5) as follows:

$$Q_o = \sum_{i=1}^{n} Q_i \tag{28}$$

The materials balance for a mixer is described as:

$$C_o = \frac{\sum_{i=1}^{n} C_i\times Q_i}{Q_o} \tag{29}$$

The outlet pressure from the mixer is the smallest inlet pressure to the mixer minus the pressure drop in the mixer.

$$P_o = \min\{P_i - \Delta P_i\},\ i = 1,2,3.....n \tag{30}$$

Where i, is the number of each stream

The pressure drop in the mixer is calculated as the pressure drop in a tee, [17]:

$$\Delta P_i = \alpha\times\rho\times\frac{V_i^2}{2} \tag{31}$$

Where:

α= 1.4 for Re ≤ 2100 and α=1 for Re > 2100

4.4. Splitter

For a specified split ratio (X), the outlet stream from splitter can be determined as shown in figure (6) by

$$Q_o = X\times Q_i \tag{32}$$

The outlet pressure is the inlet pressure minus the pressure drop in the splitter.

$$P_o = P_i - \Delta P_i \tag{33}$$

The pressure drop is calculated using equation (31)

5. RO SYSTEM's COST

For the RO system, the overall cost was defined as the total of all capital and operating cost. The cost can be calculated as follow:

$$Cost = C_{mem}A + C_{main}A + C_{pump}\left(\frac{Q_w\,\Delta P}{W_{base}\eta}\right)^n + \frac{C_{ele}Q_w\,\Delta P}{\eta} \tag{34}$$

Substituting the appropriate cost coefficients and η=0.65, [18], one obtains

$$Cost = 1.946\times10^{-3}A + 3.57\times10^{-3}A + 0.0943(0.02234Q_f\Delta P)^{0.67} + 0.08334Q_f\Delta P \quad (35)$$

6. RESULTS AND DISCUSSIONS

6.1. Effect of Feed Pressure

The feed pressure to module 1 has been changed from 40 to 150 bars. With increasing the feed pressure, the salt concentration on the membrane wall for two modules for arrangement (e) given in figure (2) was increased as illustrated in figure (7). This is attributed to the increase in both retentate concentration and permeate flux. The rate of salt concentration on the membrane wall is higher in module 1 than in module 2. This is due to the higher values of feed and retentate concentration for module 2.

A comparison between all retentate re-processing arrangements for salt concentration on wall of module 1 and module 2 is presented in figure (8). In figure (8-a), the salt concentration on membrane wall of module 1 has the same value in arrangements (a and c). This is because the feed flow rate and concentration are equal. The same trend is noticed in arrangements (d and e). The value of salt concentration on membrane wall in arrangements (a and c) is lower than that for arrangements (d, e) and all are lower than that for arrangement (b). This is because the feed flow rate in arrangements (a and c) is greater than that in arrangements (b, d and e). Figure (8-b) shows that, the differences in salt concentration on membrane wall in module 2 for arrangements (a, c, d and e) are small. However, in arrangement (b), the salt concentration on membrane wall is much smaller at lower feed pressure. This is attributed to the smaller permeate flux due to the lower net effective pressure on membrane wall.

Figure (9) illustrates the effect of feed pressure to module 1 on the salt concentration on membrane wall in module 1 for arrangement (h) given in figure (2). As the feed pressure increases, the salt concentration on membrane wall of module 1 increased. Because, higher permeate flux is obtained due to larger of net effective pressure on membrane wall. While, no significant change in salt concentration on membrane wall of module 2.

Figure (10) shows comparisons between salt concentration on membrane walls for permeate re-processing arrangements. Figure (10-a) shows that the salt concentration on membrane wall of module 1 has the same value for both arrangements (f and h). This is because the feed flow rate has small value and feed concentration is equal for arrangements (f and h). The same trend is noticed in arrangements (g and i). The value of salt concentration on membrane wall in arrangements (f and h) is smaller than that for arrangements (g and i). This is due to the smaller feed concentration. Figure (10-b) indicates the variation of salt concentration on membrane wall in module 2. The salt concentration is constant at a very small value in arrangements (f and h). Because of the small value of feed concentration, which is equal the permeate concentration for module 1. In arrangements (g and i), as the feed pressure increases, the salt concentration on membrane wall decreases, and its value for arrangement (i) is higher than that for arrangement (g).

6.2. Effect of Feed Concentration

The feed concentration has been changed from 2 to 45 kg/m^3. With increasing the feed concentration the salt concentration on membrane wall of module 1 for all retentate re-processing arrangements increases as shown in figure (11). This attributed to the increase in both feed and retentate concentration. The variation value of salt concentration on membrane wall in module 1 has the same value in arrangements (a and c). This is because the feed flow rate and concentration to these arrangements are equal. The same trend is noticed in arrangements (d and e). The value of salt concentration on membrane wall in arrangements (a and c) is lower than that for arrangements (b, d and e). This is due to the feed flow rate in arrangements (a and c) is greater than that in arrangements (b, d and e).

The variation of salt concentration on membrane wall of module 2 with feed concentration to module 1 for all retentate re-processing arrangements is shown in figure (12-a) and for all permeate re-processing arrangements is shown in figure (12-b). Figure (12-a) shows that, as the feed concentration to module 1 increases, the salt concentration on membrane wall of module 2 increases. All arrangements have the same pattern of variation. The differences in salt concentration on membrane wall of module 2 for all arrangements are small, because the differences between the feed concentration to module 2 are small. No significant change in salt concentration and its value is very small in arrangements (f and h) as shown in figure (12-b). Because the value of feed concentration to module 2 is small which is equal to the permeate concentration for module 1. In arrangements (g and i), increasing the feed concentration yield to increase the salt concentration on membrane wall of module 2. The value of salt concentration for arrangement (i) is higher than that for arrangement (g). This is due to the feed concentration for arrangement (g) is lower than that in arrangement (i).

6.3. Effect of Feed Flow Rate

The feed flow rate has been changed from 30 to 100 m^3/hr. Figure (13) shows the variation of salt concentration on membrane wall of module 1 with the feed flow rate for all retentate re-processing arrangements. It is seen that, by increasing the feed flow rate, the salt concentration on membrane wall decreases. The reason for that, as feed flow rate increases, the flow velocity increases and results in better mass transfer coefficient increases. Also the retentate concentration decreases. Thus, the salt concentration on membrane wall decreases. The arrangements (a and c) have the same value of salt concentration on membrane wall. Likewise the arrangements (d and e) have the same value of salt concentration on membrane wall. Also the arrangements (a and c) gives a lower value of salt concentration compared to the arrangements (d and c). While arrangement (b) gives a higher value of salt concentration because its have a small value of feed flow rate compared to the other arrangements.

The variation of salt concentration on membrane wall of module 2 for all retentate re-processing arrangements is presented in figure (14-a) and for all permeate re-processing arrangements as shown in figure (14-b). In figure (14-a), the salt concentration on membrane wall for module 2 decreases as the feed flow rate increases. All arrangements have the same pattern of variation and arrangement (b) gives a higher value of salt concentration. Since the feed flow rate and concentration for individual arrangement is not equal, no curve coincides with any other. In figure (14-b), the magnitude of salt concentration on membrane wall of module 2 in arrangements (f and h) is much smaller compared to (i and g). When the feed flow rate increases the salt concentration on membrane wall of module 2 is increases in arrangement (g and i). Arrangement (i) gives a higher value of salt concentration compared to arrangement (g). This is because the feed concentration to module 2 for arrangement (i) is higher than that of arrangement (g)

6.4 Effect of Feed Temperature

The feed temperature to the system has been changed from 20 to 50°C. The effect of feed temperature on salt concentration on membrane wall of module 1 for all retentate re-processing arrangements is presented in figure (15). It is clear that, as the feed temperature increases, significant decreases in the salt concentration on membrane wall occurs. Increases the feed temperature, a large change in physical properties of water, yield to large increasing in mass transfer coefficient. Thus, the salt concentration on membrane wall decreases. Arrangements (a and c) have the same value of salt concentration on membrane wall, like wise arrangements (d and e). This is because the feed flow rate to module 1 for arrangements (a and c) is equal, likewise arrangements (d and e). While arrangement (b) gives a higher salt concentration on membrane wall of module 1.

The variation of salt concentration on membrane wall of module 2 with feed temperature is presented in figures (16-a) for all retentate re-processing arrangements and (16-b) for all permeate re-processing arrangements. In figure (16-a) it is noticed that increases the feed temperature decreases the salt concentration on membrane wall of module 2. All arrangements have the same trend of variation. The salt concentration on membrane wall of module 2 in arrangement (c) is higher than that for all other arrangements. The differences between all arrangements are due to the variation of feed concentration to module 2. In figure (16-b) it is seen that no significant change in salt concentration on membrane wall of module 2 for all arrangements.

6.5 Effect of Module Dimensions

The main module dimensions are tube length, diameter and number of tubes. The total membrane area can be calculated as:

$$A = n \times \pi \times d_{ch} \times l_{ch}$$

To study the effects of module dimension on the unit performance, the length of module 1 has been changed from 0.05 to 1 m according to the membrane surface area which changed from 6.4 to 128.8 m^2.

The variation of salt concentration on membrane wall with the length of module 1 for arrangement (e) is shown in figure (17). It is clear that, as the length of module 1 increases a large increasing in salt concentration on membrane wall for module 1 while slightly increasing in salt concentration on membrane wall for module 2. As the length of module 1 increases the mass transfer coefficient for module 1 decreases, so the salt concentration on membrane wall for module 1 increases. Also the feed concentration to module 2 increases, so the salt concentration on membrane wall for module 2 is slightly increases. The effect of the channel diameter on the salt concentration on membrane wall similar to the effect of module length as shown in figure (18).

A comparison between all retentate re-processing arrangements for the length of module 1 is presented in figure (19-a) for salt concentration on membrane wall for module 1 and (19-b) for salt concentration on membrane wall for module 2. From figure (19-a) it noticed that, all arrangements have the same pattern of variation, the value of salt concentration for arrangements (a, c) is the same. This because the feed flow rate for arrangements (a and c) is the same. Also the same phenomena are observed for the arrangements (d and e). The salt concentration on

membrane wall for module 1 for arrangement (b) has the highest value. Increasing the length of module 1 increasing the feed concentration to module 2 in arrangements (a, c, d and e) thus increasing the salt concentration on membrane wall for module 2 as shown in figure (19-b). The salt concentration on membrane wall for module 2 is constant in arrangement (b) (parallel arrangement) because the feed concentration to the module 2 is equal to the feed concentration to module 1 which is constant.

Figure (20) shows the effect of length of module 1 on the salt concentration on membrane wall for arrangement (h). It is noticed that, by increasing the length of module 1 increasing the salt concentration on membrane wall for module 1 is increasing while no change in salt concentration on membrane wall for module 2 occurs. The salt concentration on membrane wall for module 1 is higher than the salt concentration on membrane wall for module 2. This because, the feed concentration to module 1 is higher than that of module 2.

A comparison between all permeate re-processing arrangement for length of module 1 is given in figure (21-a) for salt concentration on membrane wall for module 1 and figure (21-b) for salt concentration on membrane wall for module 2. Figure (21-a) presents that, the salt concentration for arrangements (g, i) has the same value because the feed flow rate is the same. This phenomenon is also observed in the arrangements (f, h). The salt concentration on membrane wall for arrangements (g, i) is higher than that arrangements (f, h). This is due to the feed flow rate to arrangement (f, h) is higher than that of arrangements (g, i). No noticed any variation in salt concentration on membrane wall for arrangements (f, h) occurs, this due to the feed concentration to module 2 which equal the permeate concentration for module 1 is very small, as illustrated in figure (21-b). Increasing the length of module 1 decreasing the salt concentration on membrane wall for arrangements (i and g). Increasing the length of module 1 increasing the permeate for module 1. When the permeate is mixed with the feed flow rate to feed modulo 2, the feed concentration decreases. Thus, the salt concentration on membrane wall decreases as well. The salt concentration on membrane wall for arrangement (i) is higher than that for arrangement (g). This is because; whole permeate for module 1 is mixed with part of feed flow rate for arrangement (g). While for arrangement (i), the part from permeate only is mixed with part of feed flow rate. Thus the feed concentration to module 2 for arrangement (g) is smaller than that for arrangement (i).

7. CONCLUSIONS

Effects of feed specifications, operating conditions and module dimensions on the concentration polarization phenomenon are studied. The following conclusions could be drawn:

1- By increasing the feed pressure, the salt concentration on membrane wall in module 1 for all arrangements is increasing.

2- As the feed concentration increases, the salt concentration on membrane wall in each module increases for all arrangements.

3- As the feed flow rate increases, the salt concentration on membrane wall in each module decreases for all retentate re-processing arrangements.

4- The increasing in the feed temperature yield to decrease in the salt concentration on membrane wall for all arrangements.

5- As the dimensions of module 1 (length and diameter) are increasing, the salt concentration on membrane wall in module 1 increases.

6- For all tested operations, no noticed any variation of salt concentration on membrane wall in module 2 for arrangements (f and h).

REFERENCES

[1] **Kalogirou S. A.,** "Seawater Desalination Using Renewable Energy Sources", Energy and Combustion Science 31, pp. 242-281, 2005.

[2] **Goosen M. F. A., Sablani S. S., Al-Hinai H., Al-Obeidani S., Al-Belushi R. and Jackson D.,** "Fouling of Reverse Osmosis and Ultrafilration Membranes: A critical Review", Speration Science and Technology, Volume 39 (10), pp. 2261-2298, 2004.

[3] **Baker, R.W.,** "Membrane Technology and Applications". McGraw-Hill, Menlo Park, 2000.

[4] **Al-Bastaki N. M. and Abbas A.,** "Modeling an industrial Reverse Osmosis Unit", Desalination 126, pp. 33-39, 1999.

[5] **Al-Bastaki N. M. and Abbas A.,** "Perdicting the Performance of RO Membranes", Desalination 132, pp. 181-187, 2000.

[6] **Kim S. and Hoek E. M. V.,** " Modeling Concentration Polarization in Reverse Osmosis Processes", Desalination 186, pp. 111–128, 2005.

[7] **Zhou W., Song L. and Guan T. K.** "A Numerical Study on Concentration Polarization and System Performance of Spiral Wound Ro Membrane Modules", Journal of Membrane Science 271, pp.38–46, 2006.

[8] **Wardeh S. and Morvan H. P.** "CFD Simulations of Flow and Concentration Polarization in Spacer-Filled Channels for Application to Water Desalination", chemical engineering research and design, 2008

[9] **Goztilvez J. M., Lora J., Mendoza J. A. and Sancho M.**, "Modeling of a Low-Pressure Reverse Osmosis System with Concentrate Recirculation to obtain High Recovery Levels". Desalination 144, pp. 341-345, 2002

[10] **jamal K., Khan M. A. and Kamil M.**, "Mathematical Modeling of Reverse Osmosis Systems". Desalination 160, pp. 29-42, 2004

[11] **Djebedjian B., Gad H., Khaled I., and Abou Rayan M.**, "An Experimental Investigation on the Operating Parameters Effecting the Performance of Reverse Osmosis Desalination System". 5th international Engineering Conference, Mansoura and Shaerm El-Shekh, March 27-31, 2006.

[12] **Elguera A. M. and Perez Baez S. O.**, "Development of the most Adequate Pre-Treatment for High Capacity Seawater Desalination Plants with Open Intake" Desalination 184, pp173–183, 2005.

[13] **H. Kotb, E. H. Amer and K. A. Ibrahim**, "Parametric Study of Retentate Re-Processing Ro Desalination Units". Engineering Research Journal, Faculty of Engineering, Minoufiya University, Egypt, Vol. 32, No. 4, October 2009.

[14] **Wilet D.E., Fell C.J.D. and Eane A.G.**, "Optimization of Membrane Module Design for Brackish Water Desalination". Desalination, (1985), Vol. 52, 249-265.

[15] **Taniguchi M., Kurihara M. and Kimura S.**, "Behavior of a Reverse Osmosis Plant Adopting a Brine Conversion Two-Stage Process and its Computer Simulation". Journal of Membrane Sciences (2001), Vol. 183, PP. 249-257.

[16] **Maskan F., Wiley D. E., Johnston L.P.M. and Celements D. J.**, "Optimal Design of Reverse Osmosis Module Networks", AICHE Journal, May (2000), Vol.46, No.5.

[17] **Warring and Horace R.**, "Valves, Piping and Pipelines Handbook". 2nd ed., Elsevier Advanced Technology, Oxford, UK, 1996.

[18] **Guria C., Bhattacharya P. K. and Gupta S. K.**, "Multi-Objective Optimization of Reverse Osmosis Desalination Units Using Different Adaptations of the Non-dominated Sorting Genetic Algorithm (NSGA)" Computers and Chemical Engineering 29, pp.1977–1995, 2005.

10. NOMENCLATURE

A	Membrane area, m^2
A_{ch}	Cross Sectional Area of the Membrane Channel, m^2
A_m	Membrane Water Permeability, m/s.kPa
A_{sh}	Cross Sectional Area of the Module's Shell Part, m^2
A_p	Cross Sectional Area of the Pipe, m^2
C_f	Feed Concentration, Kg/m^3
C_{f2}	concentration of feed water to 2nd module, Kg/m^3
C_r	Total Retentate Concentration, Kg/m^3
C_{r1}	Retentate Concentration from 1st Module, Kg/m^3
C_p	Total Permeate Concentration, Kg/m^3
C_{p1}	Permeate Concentration from 1st Module, Kg/m^3
C_w	Concentration on the Feed Side Membrane Wall, Kg/m^3
C_{p2}	Permeate Concentration from 2nd Module, Kg/m^3
C_w	Concentration on the Feed Side Membrane Wall, Kg/m^3
Cost	Total Cost , $/hr
C_{ele}	Cost Electricity ($/kWh)
C_{main}	Maintenance Cost of Membrane ($/m^2.h)
C_{mem}	Capital Cost of Membrane ($/m^2.h)
C_{pump}	Capital Cost of the Pump ($/h)
d_{ch}	Membrane Channel Diameter, m
D_s	Solute Diffusivity, m^2/s
J_s	Total Flux of Salt Permeating the Membrane, $kg/m^2.s$
j_w	Water flux, $m^3/m^2.s$
k	Mass Transfer Coefficient, m/s
L_{ch}	Length of the Membrane Channel, m
N	Number of Membrane Channels
P_{eff}	Residual Transmembrane Pressure, kPa
P_f	Feed Pressure, kPa
P_r	Retentate Pressure, kPa
Q_f	Feed Flow Rate, m^3/s
Q_{f2}	Flow Rate of Feed Water to 2nd Module, m^3/s
Q_p	Permeate flow rate , m^3/s
Q_{p1}	permeate flow rate from 1st module, m^3/s
Q_r	Retentate Flow Rate, m^3/s
Q_{r1}	Retentate Flow Rate from 1st Module, m^3/s
R	Membrane's solute rejection
Re	Reynolds number
Sc	Schmidt number (Sc value is 673-710)
T	Feed Temperature, °C
V_p	Velocity in Pipe, m/s
V_{ch}	Velocity in Membrane Channel, m/s
W_p	Energy Required to Operate the Pump, kW
X_f	Feed Split Ratio
X_r	Retentate Split Ratio
X_p	Permeate Split Ratio

Greek symbols

η	Pump Efficiency
μ	Feed Water Viscosity
π_w	Osmotic pressure on the feed side membrane wall, kPa
π_p	Osmotic pressure on the permeate side, kPa
ρ	feed side solution density, Kg/m^3
ΔP	Pressure Difference, kPa
ΔP_f	Pressure Drop due to Friction, kPa
ΔP_{in}	Pressure Drop at Inlet, kPa
ΔP_{out}	Pressure Drop at Outlet, kPa

Abbreviations

CFD	Computational Fluid Dynamics
CP	Concentration Polarization
RO	Reverse Osmosis
PH	Acidity Measure

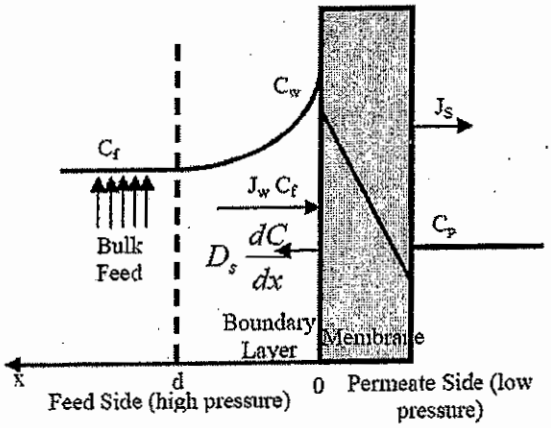

Fig. 1 Schematic Diagram of the salt Fluxes across RO Membranes, [3].

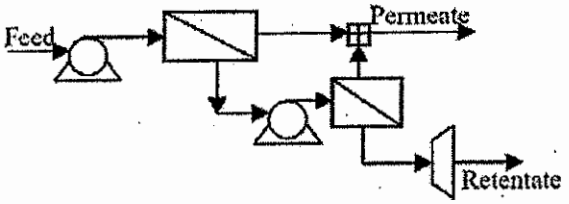

a) Series Arrangement, Retentate Re-processing

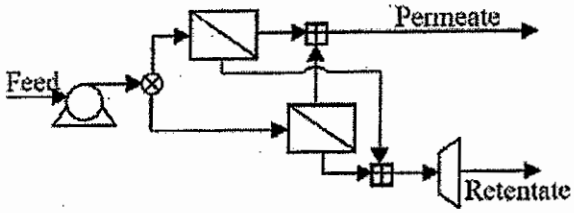

b) Parallel Arrangement

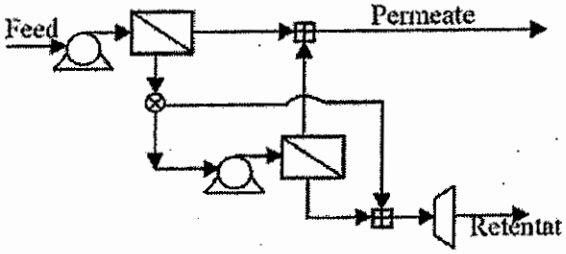

C) Series with Retentate bypass, Retentate Re-processing

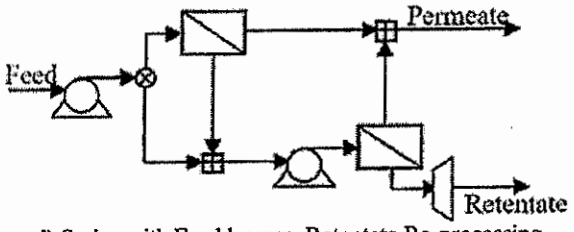

d) Series with Feed bypass, Retentate Re-processing

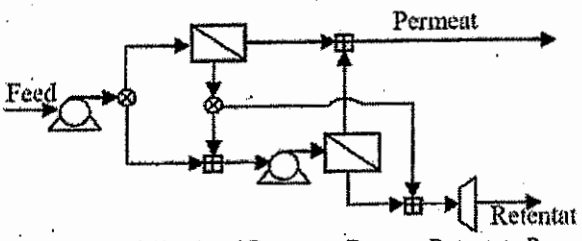

e) Series with Feed and Retentate By pass Retentate Re-processing

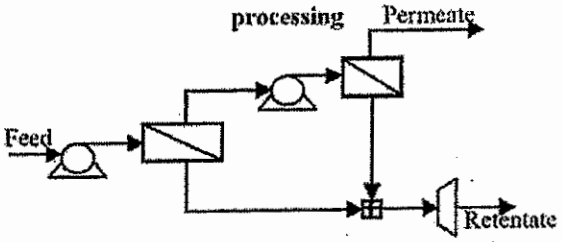

f) Series Arrangement, Permeate Re-processing

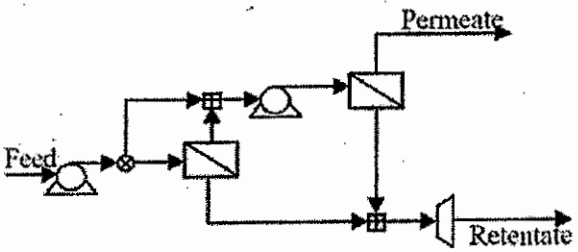

g) Series with Feed Bypass, Permeate Re-processing

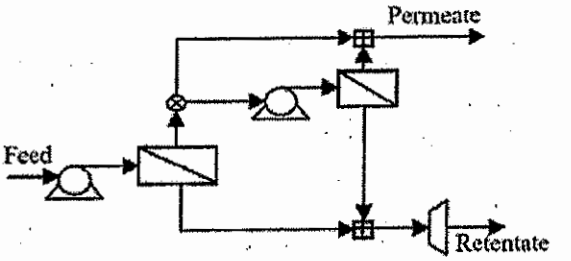

h) Series with Permeate Bypass, Permeate Re-processing

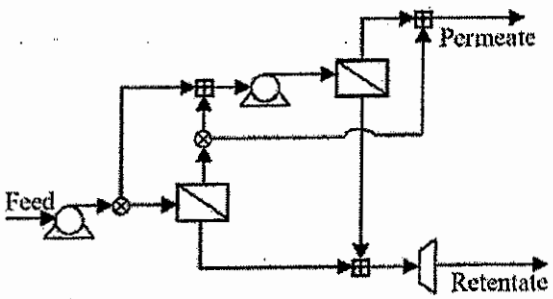

i) Series with Feed and Permeate Bypass, Permeate Re-processing

Fig. 2 Various Two Module RO Arrangements

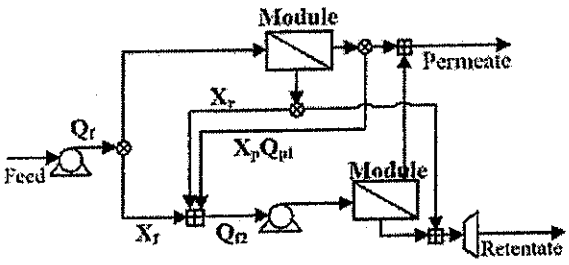

Fig. 3 Superstructure of Two-Module System

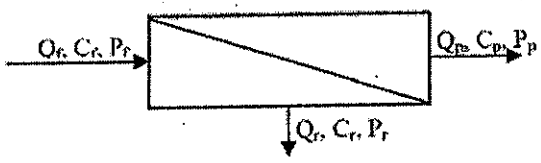

Fig. 4 Membrane Module Simulation

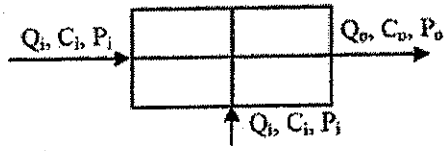

Fig. 5 Mixer Simulation

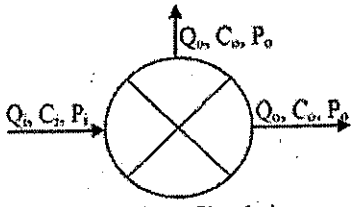

Fig. 6 Splitter Simulation

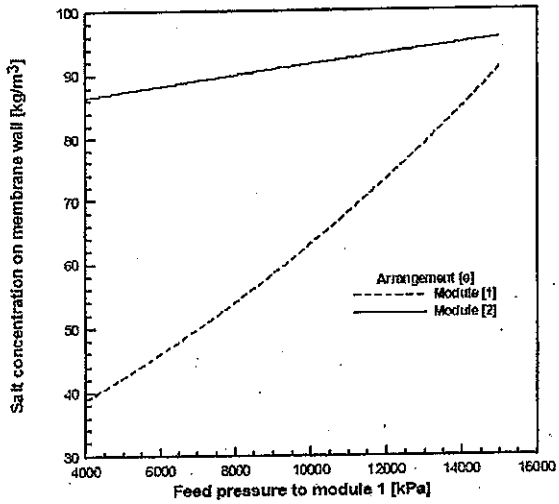

Fig. 7 Variation of salt Concentration on membrane wall with Feed Pressure to Module 1 for Arrangement [e]

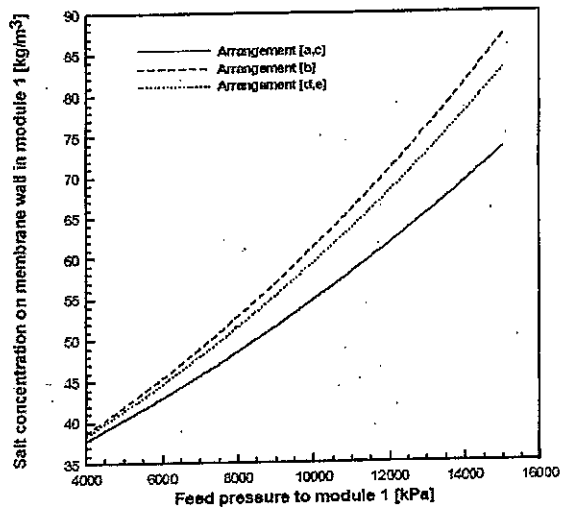

Fig. 8-a Module 1

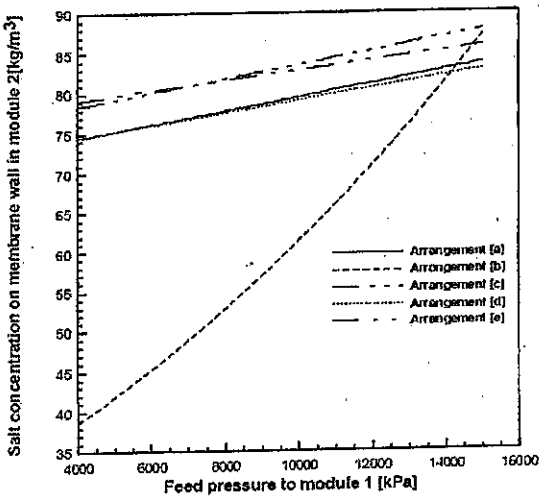

Fig. 8-b Module 2

Fig. 8 Variation of Salt Concentration on Membrane Wall with Feed Pressure to Module 1 for Retentate Re-processing Arrangements

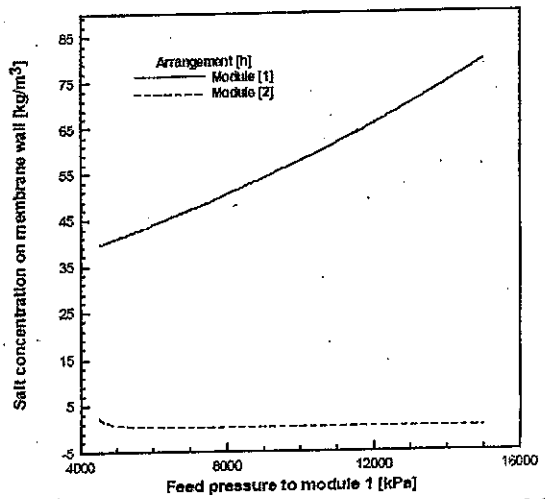

Fig. 9 Variation of Salt Concentration on Membrane Wall with Feed Pressure to Module 1 for Arrangement [h]

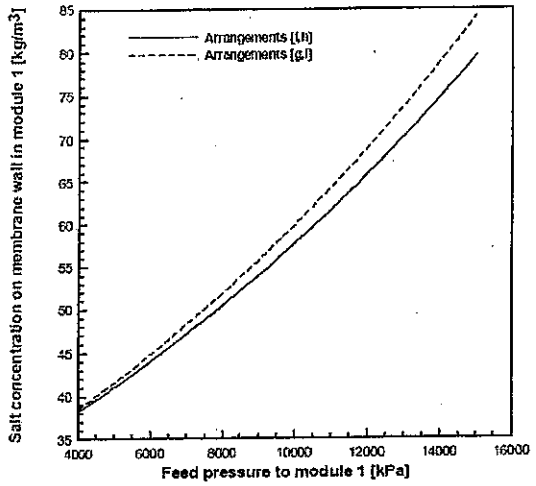

Fig.10-a. Module 1

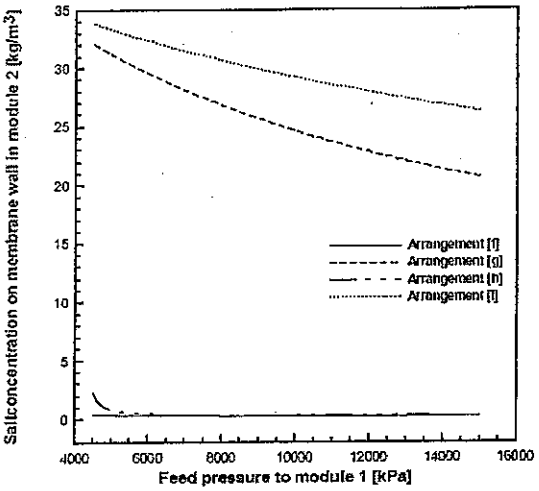

Fig.10-b Module 2

Fig.10 Variation of Salt Concentration on Membrane Wall with Feed Pressure to Module 1 for Permeate Re-processing Arrangements

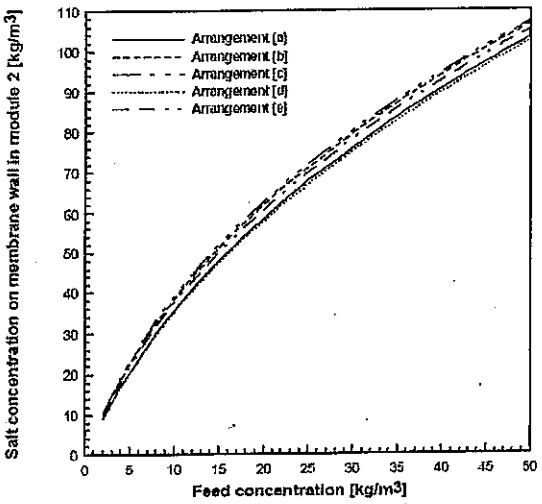

Fig. 12-a Retentate Reprocessing

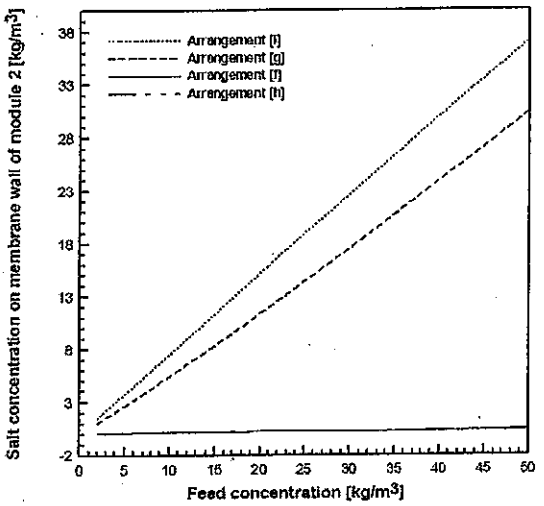

Fig.12-b Permeate Reprocessing

Fig. 12 Variation of Salt Concentration on Membrane Wall of Module 2 with Feed Concentration

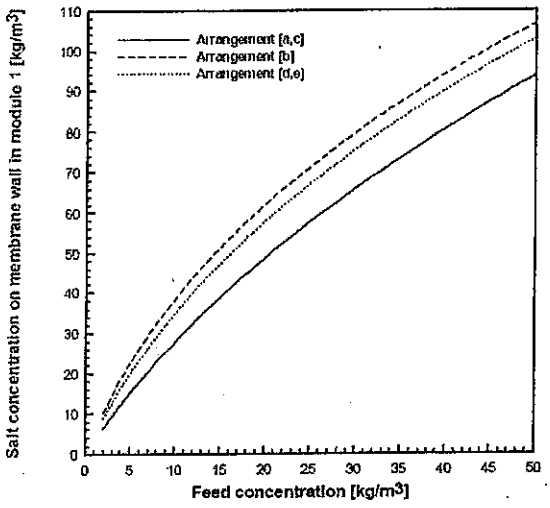

Fig.11 Variation of Salt Concentration on Membrane Wall in Module 1 with Feed Concentration for Retentate Re-processing Arrangements

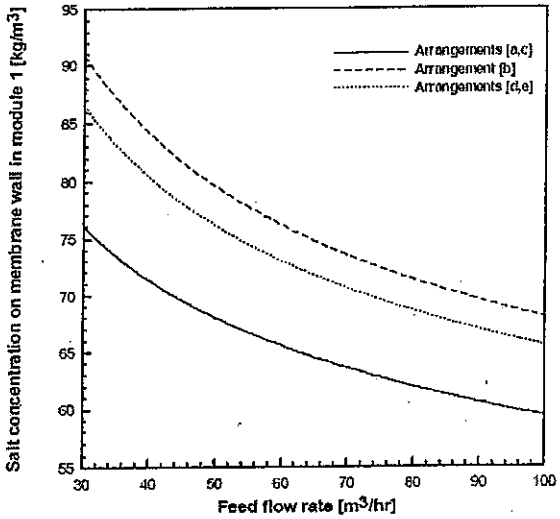

Fig.13 Variation of Salt Concentration on Membrane Wall in Module 1 with Feed Flow Rate for Retentate Re-processing Arrangements

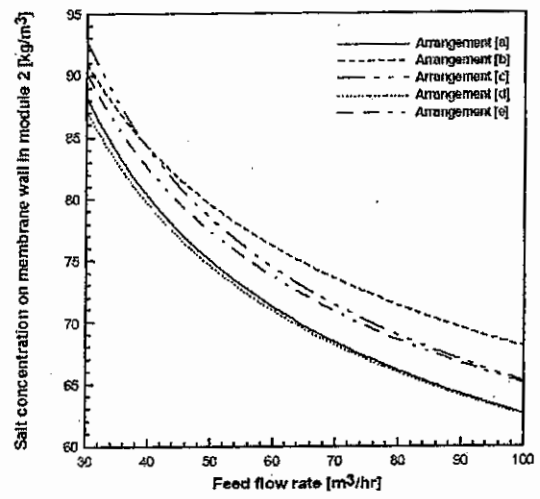

Fig.14-a Retentate Reprocessing

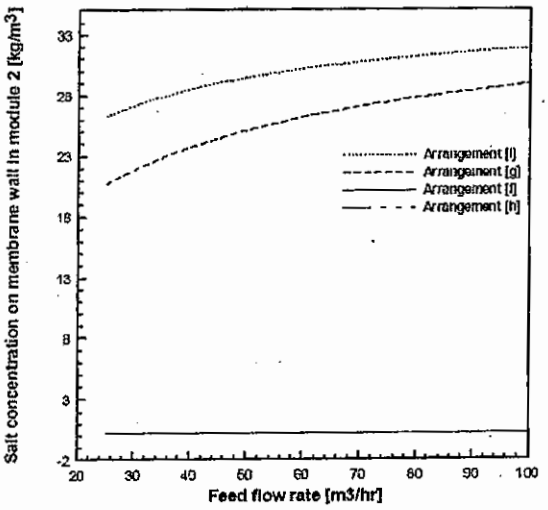

Fig. 14-b Permeate Reprocessing

Fig. 14 Variation of Salt Concentration on Membrane Wall of Module 2 with Feed Flow Rate

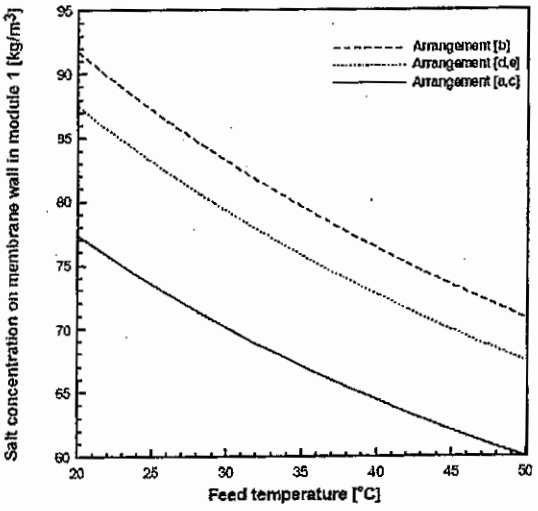

Fig.15 Variation of Salt Concentration on Membrane Wall in Module 1 with Feed Temperature for Retentate Re-processing Arrangements

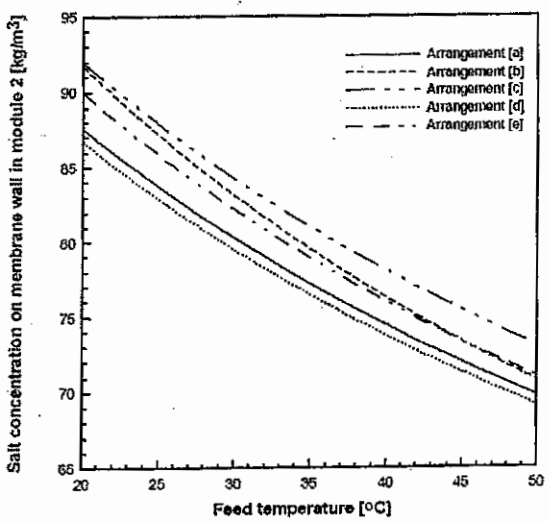

Fig. 16-a Retentate Re-processing

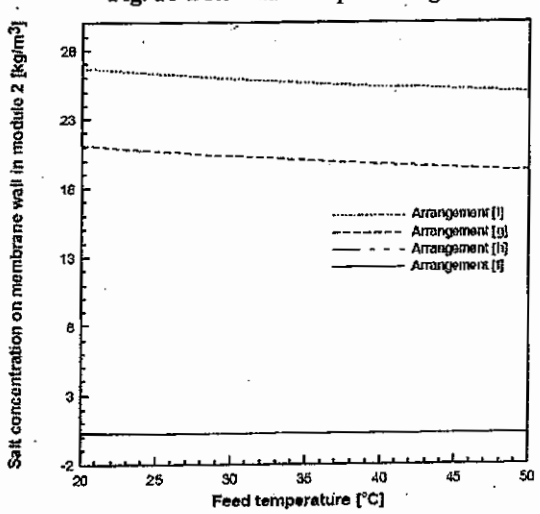

Fig.16-b Permeate Re-processing

Fig.16 Variation of Salt Concentration on Membrane Wall of Module 2 with Feed Temperature

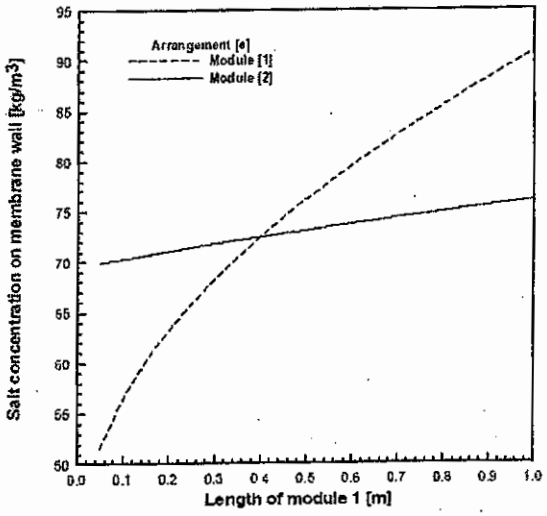

Fig. 17 Variation of Salt Concentration on Membrane Wall with Channel Length of Module 1 for Arrangement [e]

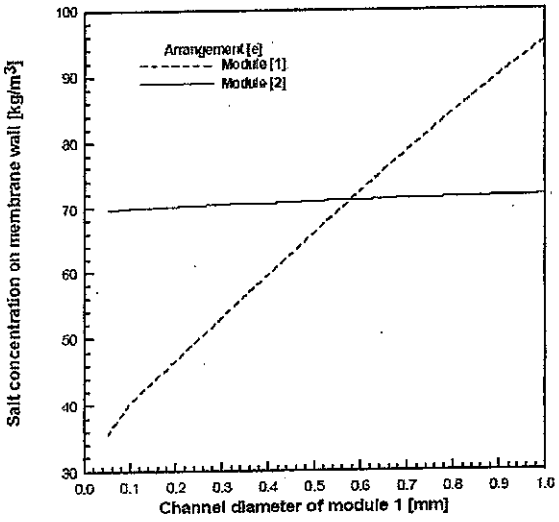

Fig.18 Variation of Salt Concentration on Membrane Wall with Channel Diameter of Module 1 for Arrangement [e]

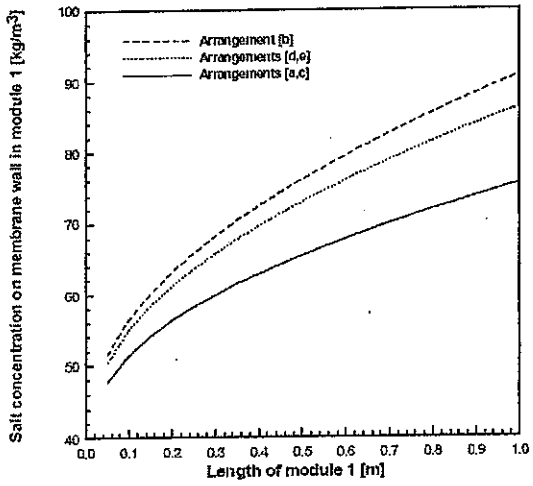

Fig.19-a. Module 1

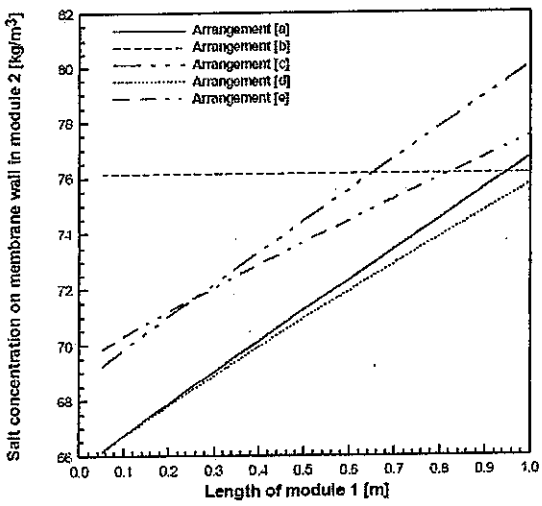

Fig.19-b Module 2

Fig.19 Variation of Salt Concentration on Membrane Wall with Channel Length of Module 1 for Retentate Re Processing Arrangements

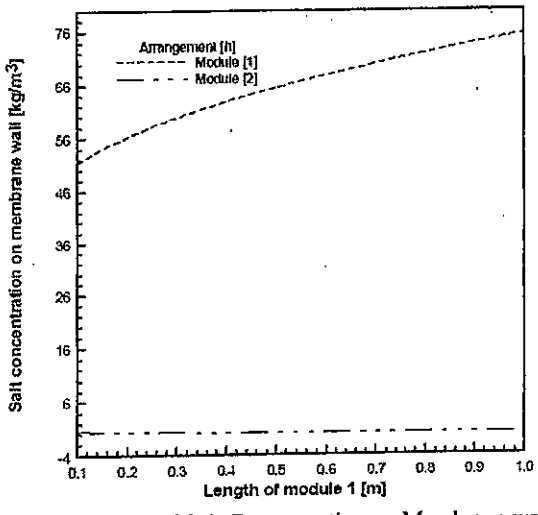

Fig. 20 Variation of Salt Concentration on Membrane wall with Length of Module 1 for Arrangement [h]

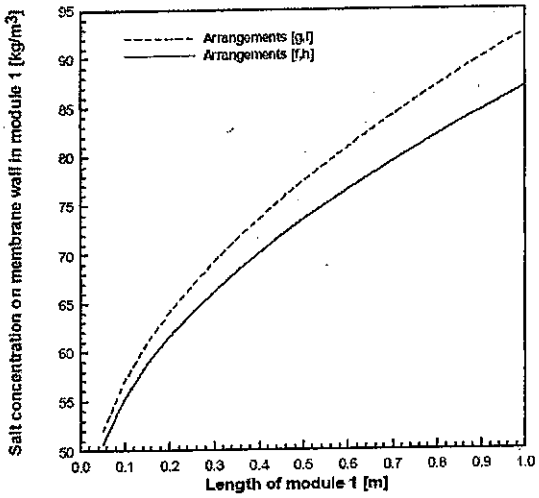

Fig. 21-a Module 1

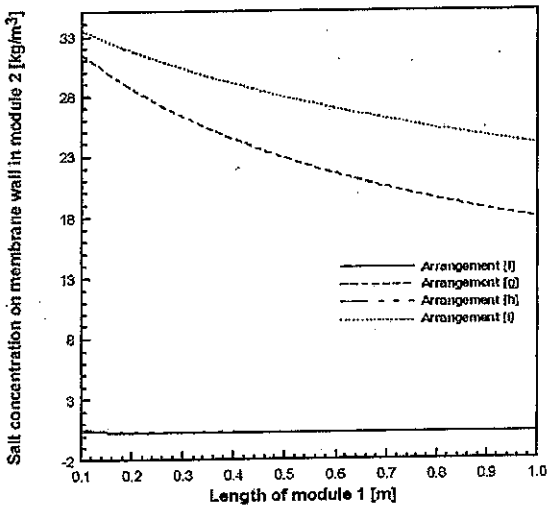

Fig. 21-b Module 2

Fig. 21 Variation of Salt Concentration on Membrane Wall with Channel Length of Module 1 for Permeate Re-Processing Arrangements

Table 1 Various Two Module RO Arrangements and their Split Ratios

Arrangement	Figure	X_f	X_r	X_p
Series, Retentate Re-processing	(1-a)	0	1	0
Parallel Arrangement	(1-b)	$0<X_f<1$	0	0
Series with Retenate Bypass, Retenate Re-processing	(1-c)	0	$0<X_r<1$	0
Series with Feed bypass, Retenate Re-processing	(1-d)	$0<X_f<1$	$X_r=1$	0
Series with Feed and Retentate Bypass, Retentate Re-processing	(1-e)	$0<X_f<1$	$0<X_r<1$	0
Series, Permeate Re-processing	(1-f)	0	0	$X_p=1$
Series with Feed Bypass, Permeate Re-processing	(1-g)	$0<X_f<1$	0	$X_p=1$
Series with Permeate Bypass, Permeate Re-processing	(1-h)	0	0	$0<X_p<1$
Series with Feed and Permeate By pass	(1-i)	$0<X_f<1$	0	$0<X_p<1$